

Sinterability of magnesium-oxide powder containing spherical agglomerates

T. MURATA, F. S. HOWELL, K. ITATANI*‡

*Department of Chemistry, Faculty of Science and Engineering, Sophia University,
7-1 Kioi-cho, Chiyoda-ku, Tokyo 102-8554, Japan*

E-mail: itatani@hoffman.cc.sophia.ac.jp

The magnesium-oxide (MgO) powders were prepared by calcining basic magnesium carbonate ($4\text{MgCO}_3 \cdot \text{Mg}(\text{OH})_2 \cdot 4\text{H}_2\text{O}$; BMC) powder at a temperature between 600°C and 1200°C for 1 to 5 h. The resulting MgO powders contained spherical agglomerates with diameters of $10\text{--}50\ \mu\text{m}$; the external shapes of these BMC agglomerates remained unchanged even after the calcination. With increasing compaction pressure, the densification of MgO powder compacts proceeded by (i) the rearrangement of agglomerates ($\leq 50\ \text{MPa}$), (ii) the collapse of agglomerates ($50\text{--}100\ \text{MPa}$), and (iii) the closer packing of primary particles ($\geq 100\ \text{MPa}$). The MgO compact was fired at 1400°C for 5 h. The relative density of the sintered MgO compact whose starting powder was prepared by calcining the BMC at 1000°C for 3 h attained 98.0%. The bending strength of this sintered MgO compact attained 214 MPa. © 2001 Kluwer Academic Publishers

1. Introduction

The sinterabilities of magnesium-oxide (MgO) powders obtained by calcining the magnesium salts have been examined by numerous researchers [1–5]. The easily-sinterable MgO powder should have the following properties [6]: (i) submicrometre-sized primary particles, (ii) narrow particle size distribution, and (iii) well-dispersed primary particles. Although the submicrometre-sized primary particles essentially show excellent sintering, they often become bridged to one another during compaction. This restricts the homogeneous packing, thereby causing inhomogeneous microstructure after sintering [7]. The granulating operation is therefore required practically to form weakly-bonded primary particles or “soft” spherical agglomerates before compaction, partly because such spherical agglomerates easily rearrange with one another during compaction to promote the homogeneous packing, and partly because such soft agglomerates are easily broken up to help closer packing of primary particles at higher compaction pressures. When the starting MgO powder already contains soft agglomerates, the granulating operation must be omitted.

Recently, basic magnesium carbonate (BMC) powder containing spherical agglomerates has been produced industrially. Since the frameworks of precursors or starting magnesium salts tend to remain immediately after the thermal decomposition [7], the soft agglomerates must be prepared without granulating operation by selecting the calcination conditions. Moreover, the

carbonate-derived MgO powder is usually sinterable [2, 7]. Based upon such background, this paper describes (i) the properties of MgO powder prepared by calcining the above BMC and (ii) the fabrication conditions of dense MgO ceramics by the pressureless sintering.

2. Experimental procedure

2.1. Starting materials

The starting powder was BMC, supplied by Ube Material Industries, Ltd (Ube, Japan). According to the manufacturer's catalogue, the purity of this BMC was over 99.5% as MgO; the kinds and amounts of impurities were CaO 72 ppm, SiO_2 86 ppm, Fe_2O_3 1 ppm, Al_2O_3 15 ppm and B_2O_3 13 ppm; the specific surface area was $35.0\ \text{m}^2 \cdot \text{g}^{-1}$. The BMC powder was calcined at the heating rate of $10^\circ\text{C} \cdot \text{min}^{-1}$ up to a temperature between 600°C and 900°C . The holding time was changed from 1 to 5 h. Hereafter the MgO powder prepared by calcining the BMC at 600°C for 1 h, for example, will be designated as MgO (600/1).

2.2. Measurements

The crystalline phase of the powder was examined using an X-ray diffractometer (XRD; Model RAD-IIA, 40 kV, 25 mA, Rigaku, Tokyo) with Ni-filtered CuK_α radiation. The differential thermal

* Author to whom all correspondence should be addressed.

‡ On sabbatical leave (1 April 2000 to 31 March 2001) from Laboratory of Solid State and Materials Chemistry, Department of Chemical Engineering and Chemistry, Eindhoven University of Technology, P.O. Box 513, 5600 MB Eindhoven, The Netherlands; E-mail: k.itatani@tue.nl

analysis (DTA) and thermogravimetry (TG) were simultaneously conducted using a DTA-TG apparatus (Model 8076D1, Rigaku, Tokyo, Japan). The specific surface area (SSA) of the resulting MgO powder was measured by a BET technique, using nitrogen (N_2) as an adsorption gas. The primary particle size was calculated on the basis of theoretical density and SSA, assuming that the particle shape was cubic. The thermal expansion-shrinkage behavior of the MgO compact was examined at the rate of $10\text{ }^\circ\text{C}\cdot\text{min}^{-1}$, using a thermomechanical apparatus (TMA; Model 8096B1, Rigaku, Tokyo, Japan). For the TMA measurement, a MgO compact with diameter of 5 mm and thickness of 3 mm was fabricated by pressing about 0.14 g of the powder uniaxially at 286 MPa. In order to measure the relative density (bulk density/theoretical density), a MgO compact with diameter of 10 mm and thickness of 3 mm was fabricated by pressing 0.40 g of the powder uniaxially at 100 MPa. Each compact was fired at $1400\text{ }^\circ\text{C}$ for 5 h. Each sintered MgO compact was polished and then thermally etched at $1350\text{ }^\circ\text{C}$ for 1 h. The bulk density was measured on the basis of mass and dimensions of the sintered MgO compact. The microstructure of the sintered MgO compact was observed using a scanning electron microscope (SEM:

Model S-430, Hitachi, Tokyo). By using the SEM micrograph, the grain sizes were measured on the basis of Fullman's correction [8].

In order to examine the mechanical strength of the sintered MgO compact, the rectangular solids with sizes of $5 \times 45 \times 3\text{ mm}^3$ were fabricated by pressing 1 g of powder uniaxially at 5 MPa and then isostatically at 100 MPa. After the solids were fired at $1400\text{ }^\circ\text{C}$ for 5 h, their three-point bending strengths were measured using a mechanical strength testing apparatus (Autostrain Model YZ-500-1-PC, Yasuda-Seiki, Tokyo, Japan).

3. Results and discussion

3.1. Properties of MgO powder

Prior to examining the properties of MgO powders, we first checked the properties of BMC powder using SEM and XRD. The SEM micrograph and X-ray powder diffraction pattern of this BMC powder are shown in Fig. 1. The SEM micrograph showed that the starting powder was composed of spherical agglomerates with diameters of 10 to $50\text{ }\mu\text{m}$. These agglomerates were furthermore composed of plate-like particles with sizes of $1\text{--}2\text{ }\mu\text{m}$ and thickness of $\sim 0.5\text{ }\mu\text{m}$ (Fig. 1a). The XRD pattern showed that only $4\text{MgCO}_3 \cdot \text{Mg}(\text{OH})_2 \cdot 4\text{H}_2\text{O}$ or

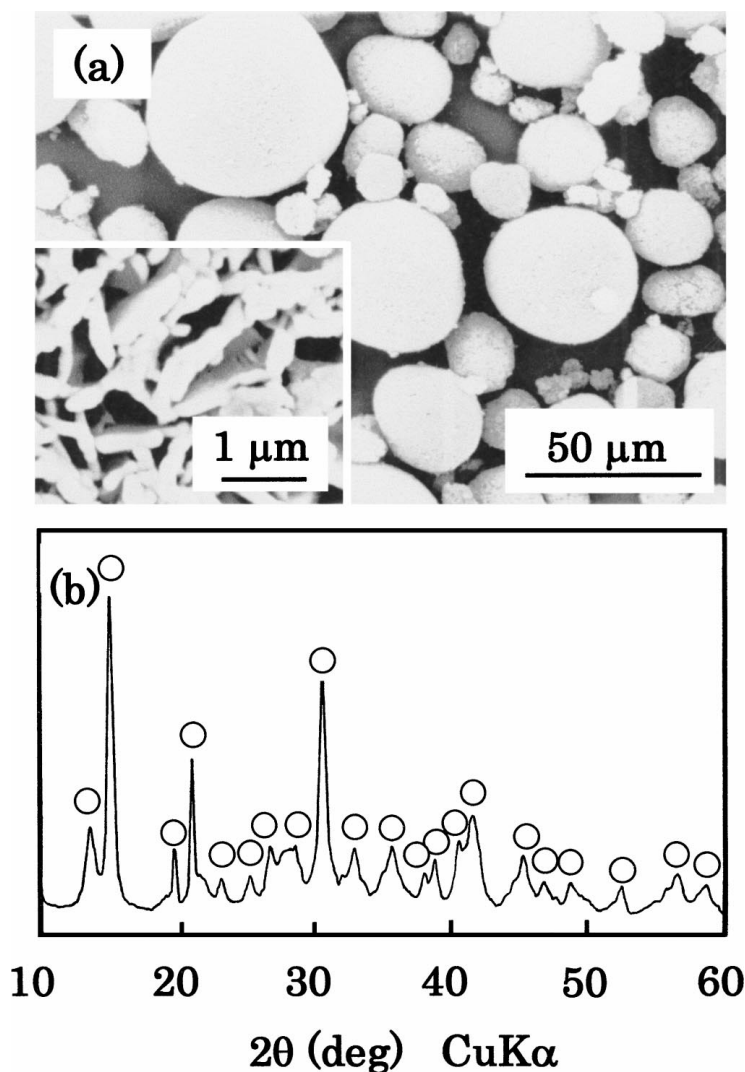


Figure 1 (a) SEM micrograph and (b) XRD pattern of BMC powder; ○: $\text{Mg}_5(\text{CCO}_3)_4(\text{OH})_2 \cdot 4\text{H}_2\text{O}$.

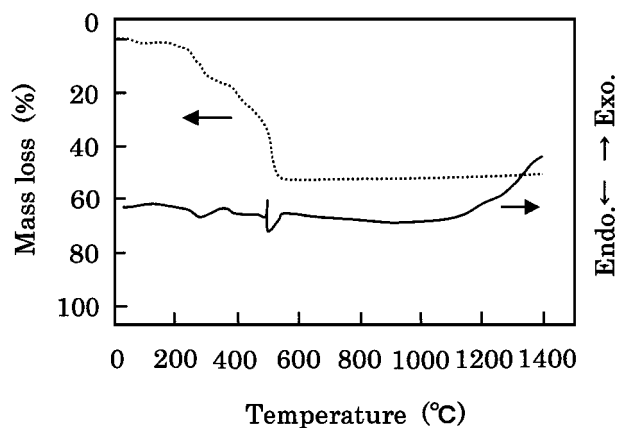


Figure 2 DTA-TG curves of BMC at the heating rate of $10^{\circ}\text{C} \cdot \text{min}^{-1}$ in air.

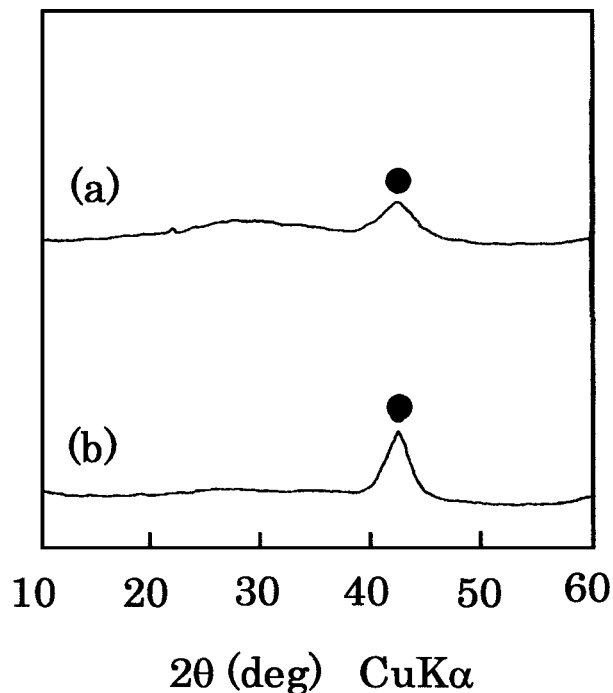


Figure 3 Typical XRD pattern after the BMC was heated at (a) 350°C and (b) 435°C ; ●: MgO.

$\text{Mg}_5(\text{CO}_3)_4(\text{OH})_2 \cdot 4\text{H}_2\text{O}$ [9] was present in the powder (Fig. 1b). The plate-like particle shapes agree well with those reported by Ainscow [10].

Next, DTA-TG analysis was conducted to make clear the formation temperature of MgO from BMC. Results are shown in Fig. 2. The DTA curve showed the endothermic effects which appeared at 250°C , 350°C and 500°C , whereas the TG curve showed the stepwise weight losses which occurred below 550°C .

The phase changes during the heating of BMC have been examined by XRD. Typical XRD patterns are shown in Fig. 3. A broad MgO reflection [11] appeared when the BMC powder was heated up to 350°C (Fig. 3a). Such MgO reflection became sharper with a further increase in temperature up to 435°C (Fig. 3b).

The thermal decomposition of BMC proceeds via the following routes: [2, 7]

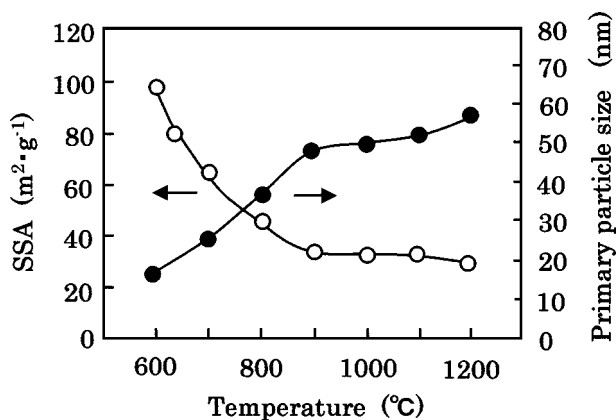
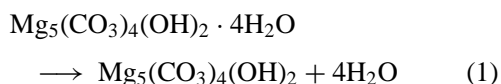


Figure 4 Typical changes in SSA and primary particle size of the MgO powder with calcination temperature. Calcination time: 3 h.

On the basis of the present data, the endothermic effect which appeared at 250°C may be attributed to the release of H_2O (Equation 1). On the other hand, the endothermic effects at 350°C and 500°C are ascribed to the thermal decomposition of $\text{Mg}_5(\text{CO}_3)_4(\text{OH})_2$ to form MgO with releasing H_2O and CO_2 (Equation 2), although the decomposition process does not appear to be simple [12].

The results suggest that MgO powder is obtained by calcining the BMC above 500°C . On the basis of this information, MgO powders were prepared by calcining the BMC at a temperature between 600°C and 1200°C . The calcination time was changed from 1 to 5 h at each temperature.

The SSAs of these MgO powders were examined. Typical results of MgO powders calcined for 3 h are shown in Fig. 4, together with primary particle size. The overall trend revealed that the SSA value of MgO powder was reduced and primary particle size was enhanced with calcination temperature. Although the data on MgO powders calcined for 1 h and 5 h were omitted in this paper, the SSA values of MgO powders calcined for 1 h were about 1.2 times higher but those calcined for 5 h were almost the same compared to those calcined for 3 h. On the other hand, the primary particle sizes were classified, according to the calcination time as follows: $3 \text{ h} \approx 5 \text{ h} > 1 \text{ h}$.

The decreasing of SSA with calcination temperature may be ascribed to the primary particle growth of MgO. If one compares with the primary particle sizes at fixed temperatures, the primary particle sizes for the calcination time of 3 h are almost the same as those for 5 h. This fact indicates that no appreciable primary particle growth of MgO occurs when the calcination time exceeds 3 h.

The changes in particle shape with calcination temperature were examined using SEM. Typical results on high and low magnification micrographs of MgO(1000/3) powder are shown in Fig. 5. The MgO(1000/3) powder was composed of spherical agglomerates with diameters of 10 to $50 \mu\text{m}$. The individual particle shapes were spherical and particles diameters were $\sim 0.1 \mu\text{m}$.

Although no changes in agglomerate shape were observed compared to the case of BMC (see Fig. 1), the particle shape changes from plate-like to spherical.

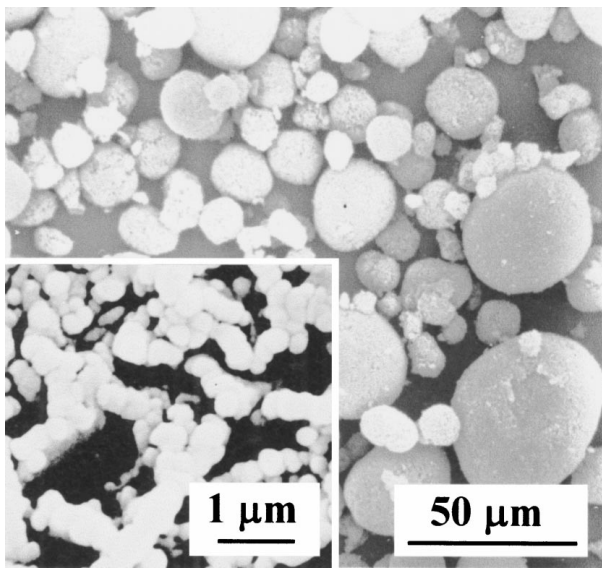


Figure 5 SEM micrographs of MgO(1000/3) powder. Note that the high magnification and low magnification images are shown in the figure.

Such plate-like particles still remained at 600–800 °C (data are not shown here). These plate-like particles may be “pseudomorphs” of the original BMC. The pseudomorphs appear to collapse at ~1000°C, due to the primary particle growth of MgO. On further increase in calcination temperature, the sintering of primary particles makes the collapse of agglomerates difficult [2, 7].

In order to fabricate the dense MgO compact having homogeneous microstructure, the densification process of MgO powder compact was examined as a function of compaction pressure. Typical results of MgO(1000/3) compact are shown in Fig. 6, together with SEM micrographs. Although the relative density of MgO(1000/3) compact was below 20% at 15 MPa, it increased with pressure and attained ~60% at 200 MPa. The density-pressure curve contained two break points at ~50 and ~100 MPa. SEM micrographs showed that the spherical agglomerates with diameters of 10 to 50 μm were closely packed at 20 MPa. Most of the agglomerates disappeared when the pressure was raised up to 100 MPa. The microstructure of MgO compact at 200 MPa was similar to that of MgO compact pressed at 100 MPa.

The dotted line in the figure indicates the compaction behaviour of MgO powder (average primary particle size: 49 nm) prepared by vapour phase oxidation process (VPO) [13]. Since the VPO-derived MgO powder is prepared by the reaction between Mg vapour and oxygen, i.e., the “build-up” process of MgO crystals, it is composed of well-dispersed primary particles. In the compaction range of 40 to 100 MPa, the relative densities of the present MgO compacts are similar to those of VPO-derived MgO powder compacts. This fact suggests that the present spherical agglomerates may collapse to help closer packing of primary particles. On the basis of the data on density-pressure curves and SEM micrographs, the present MgO powder may be densified

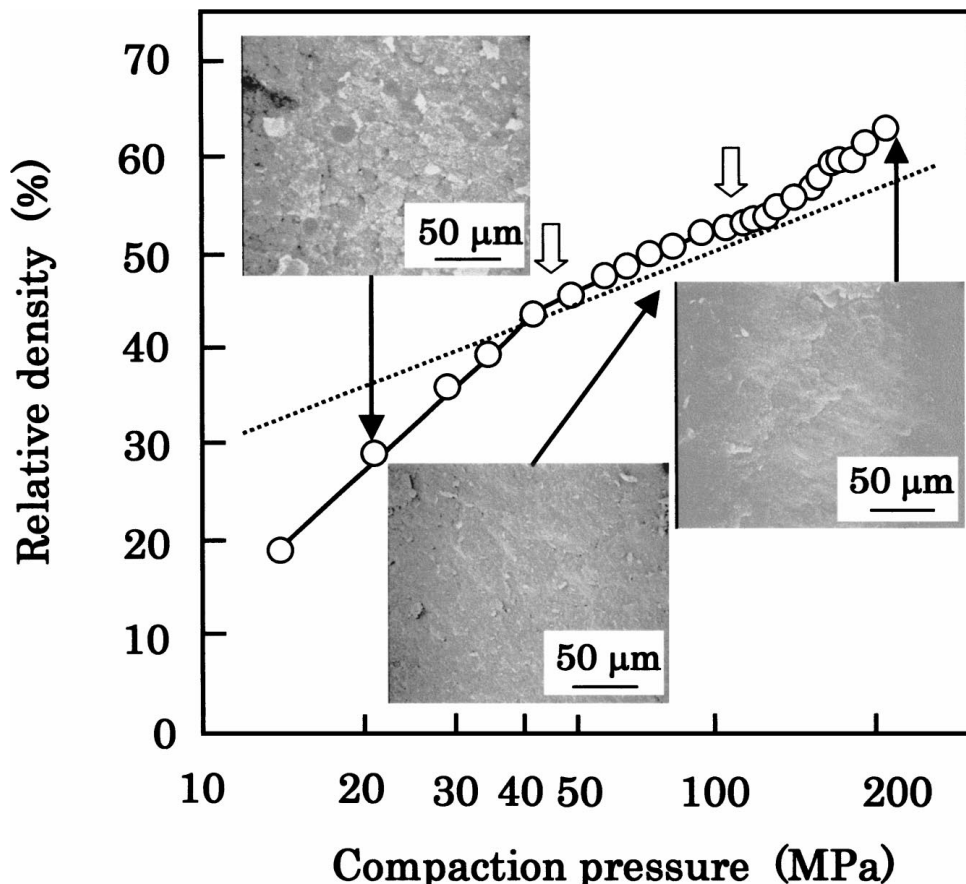


Figure 6 Changes in relative density of MgO(1000/3) compact with compaction pressure, together with SEM micrographs. Arrow marks indicate the break points of the lines. The dotted line shows the densification behaviour of MgO powder prepared by VPO [13].

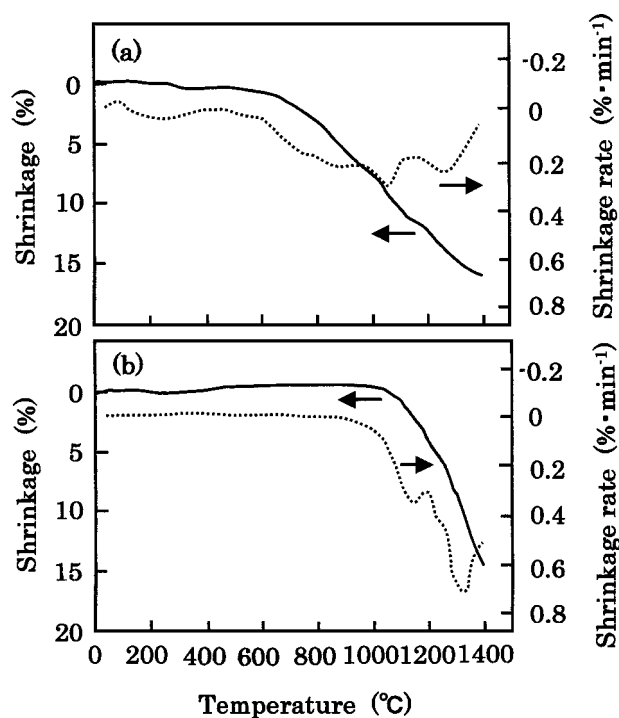


Figure 7 Typical expansion-shrinkage curves and differential (shrinkage rate) curves of (a) MgO(600/3) and (b) MgO(1000/3) compacts at the heating rate of $10\text{ }^{\circ}\text{C}\cdot\text{min}^{-1}$.

along with the following processes: (i) the spherical agglomerates are rearranged toward the closer packing at compaction pressures of $\lesssim 50$ MPa; (ii) the agglomerates are collapsed to help closer packing of primary particles at pressures of 50 to 100 MPa; (iii) the primary particles are closer packed at $\gtrsim 100$ MPa.

3.2. Sintering of MgO powder

3.2.1. Sintering at increasing temperatures

The sinterabilities of MgO powders prepared by calcining the BMC at a temperature between $600\text{ }^{\circ}\text{C}$ and $1000\text{ }^{\circ}\text{C}$ are presented in this section. First, the thermal expansion-shrinkage behaviours of these MgO powders were examined to make clear the densification process. Typical results on the thermal expansion-shrinkage curves of MgO(600/3) and MgO(1000/3) compacts are shown in Fig. 7, together with the differential shrinkage (= shrinkage rate) curves. The shrinkage of MgO(600/3) compact started at around $600\text{ }^{\circ}\text{C}$ and proceeded with temperature. The shrinkage-rate curve of this MgO compact contained minima at around $700\text{ }^{\circ}\text{C}$ (broad), $900\text{ }^{\circ}\text{C}$ (broad), $1100\text{ }^{\circ}\text{C}$ and $1300\text{ }^{\circ}\text{C}$ (Fig. 7a).

The shrinkage of MgO(1000/3) compact started at around $1000\text{ }^{\circ}\text{C}$ and proceeded with temperature. The shrinkage-rate curve of this MgO compact contained two distinct minima at around $1100\text{ }^{\circ}\text{C}$ and $1300\text{ }^{\circ}\text{C}$ (Fig. 7b).

The microstructural changes during the heating of MgO(600/3) and MgO(1000/3) compacts were examined using the SEM. Typical SEM micrographs of these MgO compacts are shown in Fig. 8. The SEM micrographs of MgO(600/3) compact showed that pores were present along the spherical grains at $1000\text{ }^{\circ}\text{C}$, and

that irregularly shaped pores remained on boundaries of grains with sizes of $\sim 5\text{ }\mu\text{m}$ at $1400\text{ }^{\circ}\text{C}$. The SEM micrographs of MgO(1000/3) compact showed that spherical grains with diameters of $\sim 0.2\text{ }\mu\text{m}$ were closely packed at $1000\text{ }^{\circ}\text{C}$, and that grains with sizes of $\sim 1\text{ }\mu\text{m}$ were closely packed at $1400\text{ }^{\circ}\text{C}$.

The shrinkage-rate curve of MgO (600/3) compact contains several minima, which suggests that the difference in sintering rates between primary particles and agglomerates may form the inhomogeneous microstructure. On the other hand, the shrinkage-rate curve of MgO (1000/3) compact includes two distinct minima at around $1100\text{ }^{\circ}\text{C}$ and $1300\text{ }^{\circ}\text{C}$. The phenomenon at $1100\text{ }^{\circ}\text{C}$ corresponds to the sintering of primary particles to form grains, whereas the phenomenon at $1300\text{ }^{\circ}\text{C}$ corresponds to the elimination of pores from the system, due to the sintering of grains. These two distinct minima in the shrinkage-rate curve demonstrate that the primary particles may be sintered homogeneously, chiefly because no strongly-bonded primary particles or “hard” agglomerates are present in the starting compact.

3.2.2. Sintering at fixed temperatures

On the basis of the information in Section 3.2.1, the relative densities of these MgO compacts fired at $1400\text{ }^{\circ}\text{C}$ for 5 h were examined. The compaction pressure was selected to be 100 MPa, because most of the agglomerates were collapsed at this pressure. The relative densities of sintered MgO compacts are plotted against calcination temperature. Results are shown in Fig. 9. The overall trend revealed that the relative densities of sintered MgO compacts increased with calcination temperature and attained maxima at $1000\text{ }^{\circ}\text{C}$; however, they decreased with a further increase in calcination temperature. The relative densities of MgO compacts were classified as follows: $3\text{ h} \approx 1\text{ h} \gtrsim 5\text{ h}$. The relative density of MgO(1000/3) compact attained a maximum (98.0%).

The present authors have examined the sinterabilities of commercially-available MgO powders prepared by various processes, i.e., sea-water magnesia, spark-discharge and VPO processes [5]. Although these MgO powder compacts are pressureless sintered at $1450\text{ }^{\circ}\text{C}$ for 5 h, the relative densities are $\sim 95\%$. The relative densities as high as 98% may be obtained when the VPO-derived MgO powder compacts are pressureless sintered at $1700\text{ }^{\circ}\text{C}$ for 5 h [14].

The microstructures of these sintered MgO compacts were examined using SEM. A typical SEM micrograph of sintered MgO(1000/3) compact is shown in Fig. 10, together with grain size distribution. The polyhedral grains were closely packed in the sintered compact (Fig. 10a). The grain size distribution showed that the grain sizes were distributed over the range of 5 to $70\text{ }\mu\text{m}$; the average grain size was estimated to be $17.5\text{ }\mu\text{m}$ (Fig. 10b).

The relationship between relative density and calcination temperature shows that the optimum calcination temperature and time for the highest relative density of sintered MgO compact are $1000\text{ }^{\circ}\text{C}$ and 3 h,

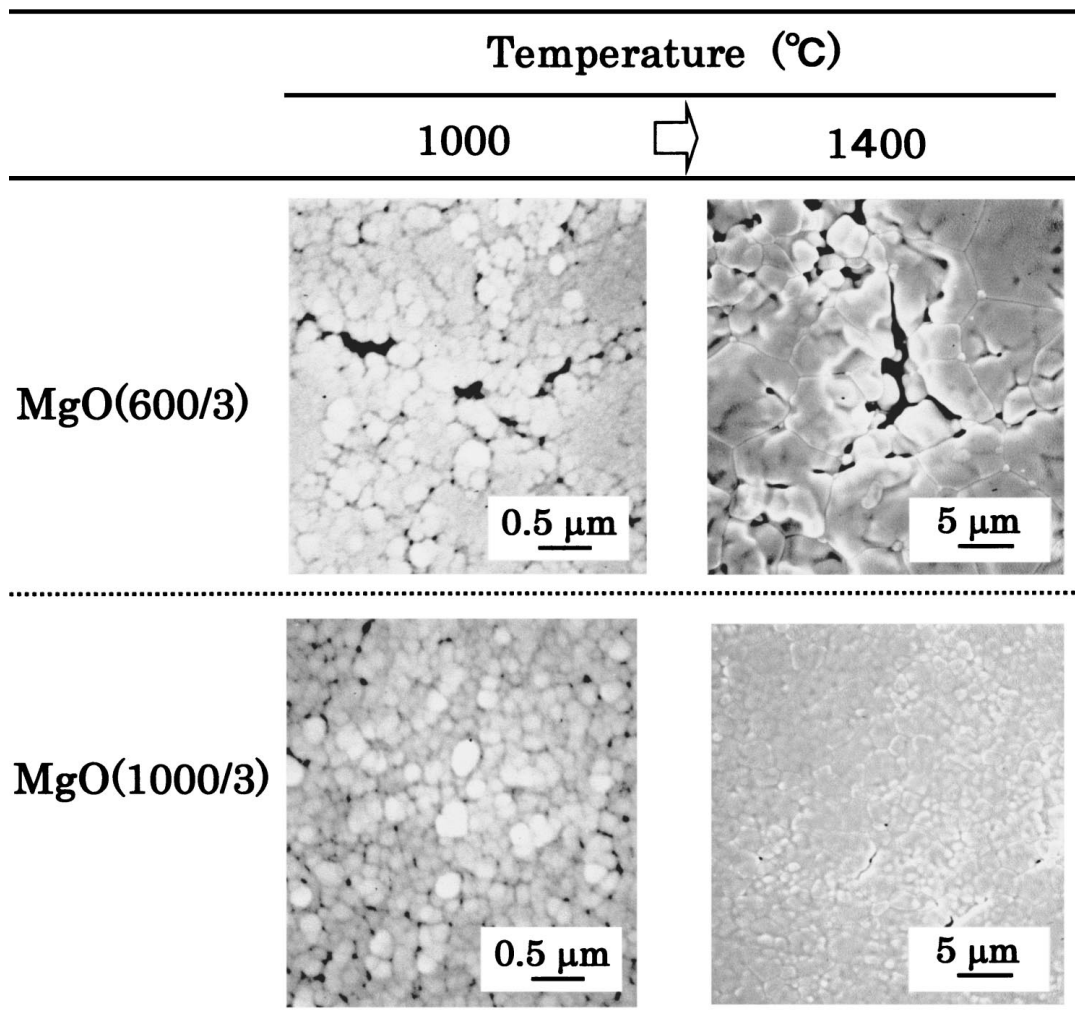


Figure 8 Typical SEM micrographs during the heating of MgO(600/3) compact and MgO(1000/3) compact.

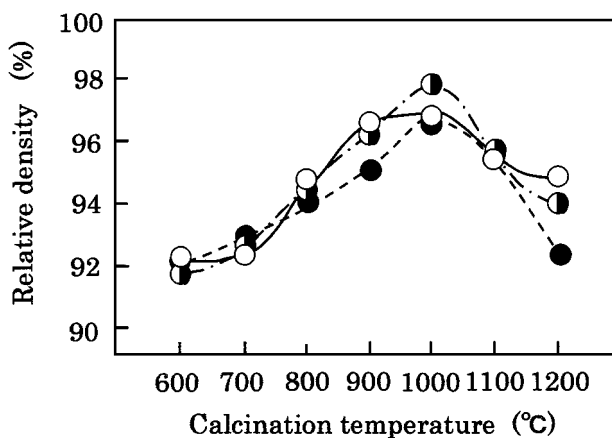


Figure 9 Relationship between calcination temperature and relative density of MgO (1000/3) compact fired at 1400°C for 5 h. Calcination time: ○—○: 1 h; ○- - -○: 3 h; ●·····●: 5 h.

respectively. When the calcination temperatures are below 1000 °C, the densification may be retarded by the presence of pores not only on grain boundaries but also within grains, chiefly due to the inhomogeneous sintering in the presence of hard agglomerates (see Fig. 8). When the calcination temperature exceeds 1000 °C, the densification of MgO compact may be delayed, chiefly

due to a lowering of the driving force for sintering by the primary particle growth.

The three-point flexural strength of sintered MgO(1000/3) compact was measured. The average flexural strength was 214 MPa. The fractured surfaces of this sintered MgO(1000/3) compact were observed using SEM. Some grains appeared to be smooth, but others to be convex. The smooth grains indicate the propagation of transgranular cracks, whereas the convex grains suggest the propagation of intergranular cracks.

The flexural strength (214 MPa) of sintered MgO(1000/3) compact with average grain size of 17.5 μm is higher than the strength (~170 MPa) of VPO-derived MgO powder compact with average grain size of ~20 μm [14]. This fact suggests that the present MgO compact possesses more homogeneous microstructure than the VPO-derived MgO compact, because there are no appreciable differences in relative density and grain size between these two MgO compacts. Our explanation of transgranular and intergranular crack propagation may be supported by Rice [15], who pointed out that the fracturing mode in the case of the grain sizes of around 20 μm may include 20–60% of intergranular fracturing and 40–80% of transgranular fracturing.

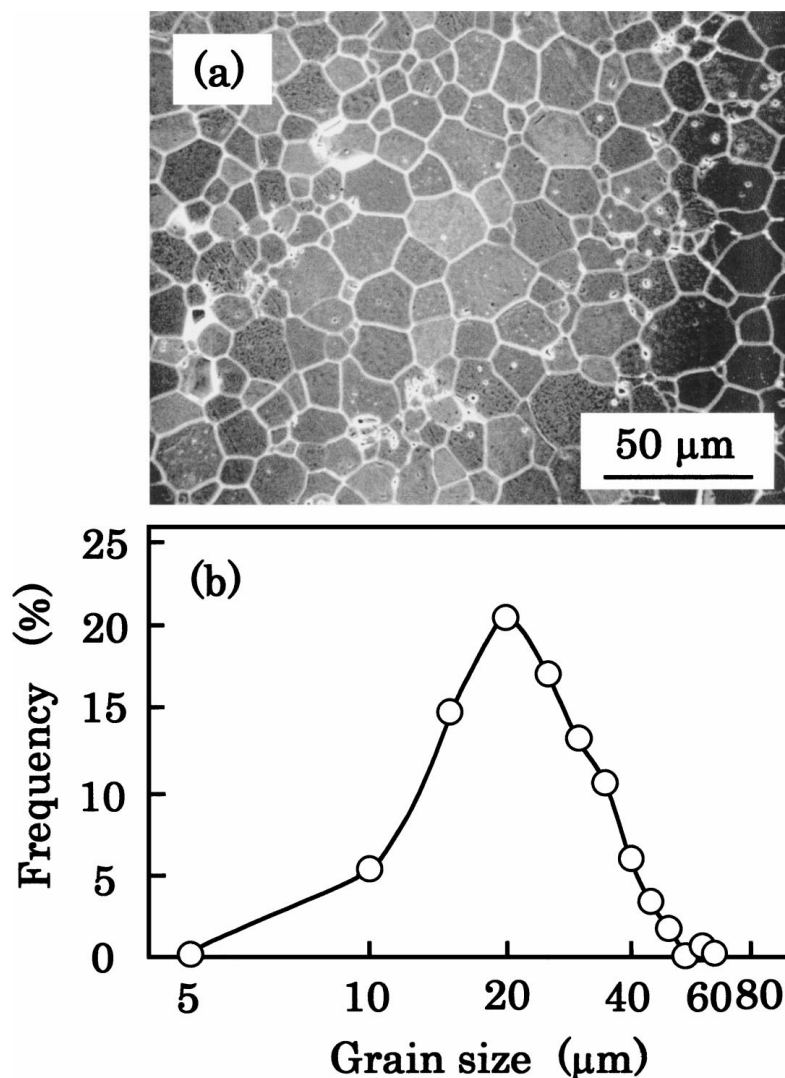


Figure 10 Typical (a) SEM micrograph and (b) grain size distribution of MgO(1000/3) compact fired at 1400 °C for 5 h.

4. Conclusion

The sinterabilities of MgO powders prepared by calcining the basic magnesium carbonate ($\text{Mg}_5(\text{CO}_3)_4(\text{OH})_2 \cdot 4\text{H}_2\text{O}$; BMC) were examined. The results obtained can be summarized as follows:

(i) The BMC powder contained spherical agglomerates with diameters of 10–50 μm. This powder was calcined at a temperature between 600 °C and 1200 °C to form MgO powder. The resulting MgO powders were composed of spherical agglomerates. Such external shapes of spherical agglomerates remained unchanged without collapse even after the calcination. With increasing compaction pressure, the homogeneous packing of primary particles was accomplished above 100 MPa, along with the routes of the rearrangement of agglomerates (≤ 50 MPa) and the collapse of agglomerates (50 to 100 MPa).

(ii) The MgO compact was fired at 1400 °C for 5 h. The relative density of a sintered MgO compact whose starting powder was prepared by calcining the basic magnesium carbonate at 1000 °C for 3 h attained 98.0%. The bending strength of this sintered compact was 214 MPa. The polyhedral grains with the average

grain size of 17.5 μm were closely packed in the sintered compact.

Acknowledgements

The authors wish to express their thanks to Ube Material Industries, Ltd. for providing the basic magnesium carbonate.

References

1. W. H. RHODES and B. J. WENCH, *J. Amer. Ceram. Soc.* **56** (1973) 495.
2. K. HAMANO, Z. NAKAGAWA and H. WATANABE, *Mater. Sci. Monogr.* **14** (1982) 159.
3. J. GREEN, *J. Mater. Sci.* **18** (1983) 637.
4. C. ZOGRAFOU and E. NAUJOKAT, *Keram. Zeit.* **37** (1985) 454.
5. K. ITATANI, M. NOMURA, A. KISHIOKA and M. KINOSHITA, *J. Mater. Sci.* **21** (1986) 1429.
6. K. ITATANI, A. ITOH, F. S. HOWELL, A. KISHIOKA and M. KINOSHITA, *ibid.* **28** (1993) 719.
7. K. HAMANO, *Taikabutsu* **37** (1985) 124.
8. R. L. FULLMAN, *Trans. AIME* **197** (1953) 447.
9. Powder Diffraction File Card No. 25-513, JCPDS International Center for Diffraction Data, Newtown Square, PA (1975).
10. W. S. AINSCOW, *Refr. J.* **May/June** (1984) 6.

11. Powder Diffraction File Card No. 4-829, JCPDS International Center for Diffraction Data, Newtown Square, PA (1954).
12. Y. SAWADA, K. UEMATSU, N. MIZUTANI and M. KATO, *Nihon-Kagaku-Kaishi* **1979** (1979) 57.
13. A. NISHIDA, K. YOSHIDA and W. KOBAYASHI, *Adv. Ceram.* **21** (1987) 271.
14. A. ITOH, K. ITATANI, F. S. HOWELL, A. KISHIOKA and M. KINOSHITA, *J. Mater. Sci.* **31** (1996) 2757.
15. R. W. RICE, *Proc. Brit. Ceram. Soc.* **20** (1972) 329.

*Received 14 January
and accepted 15 September 2000*